



HAL
open science

Tissue no-reflow despite full recanalization following thrombectomy for anterior circulation stroke with proximal occlusion: A clinical study

Adrien Ter Schiphorst, Sylvain Charron, Wagih Ben Hassen, Corentin Provost, Olivier Naggara, Joseph Benzakoun, Pierre Seners, Guillaume Turc, Jean-Claude Baron, Catherine Oppenheim

► To cite this version:

Adrien Ter Schiphorst, Sylvain Charron, Wagih Ben Hassen, Corentin Provost, Olivier Naggara, et al.. Tissue no-reflow despite full recanalization following thrombectomy for anterior circulation stroke with proximal occlusion: A clinical study. *Journal of Cerebral Blood Flow and Metabolism*, 2020, pp.271678X20954929. 10.1177/0271678X20954929 . inserm-02978221

HAL Id: inserm-02978221

<https://inserm.hal.science/inserm-02978221v1>

Submitted on 26 Oct 2020

HAL is a multi-disciplinary open access archive for the deposit and dissemination of scientific research documents, whether they are published or not. The documents may come from teaching and research institutions in France or abroad, or from public or private research centers.

L'archive ouverte pluridisciplinaire **HAL**, est destinée au dépôt et à la diffusion de documents scientifiques de niveau recherche, publiés ou non, émanant des établissements d'enseignement et de recherche français ou étrangers, des laboratoires publics ou privés.

Tissue no-reflow despite full recanalization following thrombectomy for anterior circulation stroke with proximal occlusion: a clinical study

Adrien ter Schiphorst^{1,2}, MD; Sylvain Charron^{1,3}, PhD; Wagih Ben Hassen^{1,3}, MD; Corentin Provost^{1,3}, MD; Olivier Naggara^{1,3}, PhD; Joseph Benzakoun^{1,3}, MD; Pierre Seners^{1,4}, PhD; Guillaume Turc^{1,4}, PhD; Jean-Claude Baron^{1,4*}, MD, ScD; Catherine Oppenheim^{1,3*}, PhD.

1. INSERM U1266, Université de Paris, France

2. Department of Neurology, CHU Montpellier, University of Montpellier, France

3. Department of Neuroradiology, Hôpital Sainte-Anne, Université de Paris, France

4. Department of Neurology, Hôpital Sainte-Anne, Université de Paris, France.

*These authors contributed equally to this work

Cover title: Tissue no-reflow despite full recanalization

Corresponding author: Jean-Claude Baron, Department of Neurology, Hôpital Sainte-Anne, 75014 Paris, France;

E-mail address: jean-claude.baron@inserm.fr; tel: +33145656268

Word count: 4762 (including Abstract)

Figures: 3

Tables: 3

Supplemental material: 2 tables, 1 figure

Key-words: perfusion; cerebral blood flow; arterial spin labelling; large vessel occlusion; cerebral infarction

Abstract

Despite early thrombectomy, a sizeable fraction of acute stroke patients with large vessel occlusion have poor outcome. The no-reflow phenomenon, i.e., impaired microvascular reperfusion despite complete recanalization, may contribute to such ‘futile recanalizations’. Although well reported in animal models, no-reflow is still poorly characterized in man. From a large prospective thrombectomy database, we included all patients with intracranial proximal occlusion, complete recanalization (modified thrombolysis in cerebral infarction score 2c-3), and availability of both baseline and 24h follow-up MRI including Arterial Spin Labelling perfusion mapping. No-reflow was operationally defined as hypoperfusion $\geq 40\%$ relative to contralateral homologous region, assessed with both visual (two independent investigators) and automatic image analysis, and infarction on follow-up MRI. Thirty-three patients were eligible (median age: 70yrs, NIHSS: 18, stroke onset-to-recanalization delay: 208min). The operational criteria were met in one patient only, consistently with the visual and automatic analyses. This patient recanalized 160min after stroke onset and had excellent functional outcome. In our cohort of patients with complete and stable recanalization following thrombectomy for intracranial proximal occlusion, severe ipsilateral hypoperfusion on follow-up imaging associated with newly developed infarction was a rare occurrence. Thus, no-reflow may be infrequent in human stroke and may not substantially contribute to futile recanalizations.

Introduction

In acute ischemic stroke (AIS) due to large vessel occlusion (LVO), mechanical thrombectomy preceded or not by intravenous thrombolysis affords >80% recanalization rates and significantly improves outcome¹. However, >50% of treated patients do not recover to an independent life¹. Understanding the mechanisms underlying such ‘futile recanalizations’² may lead to novel therapies as adjuncts to thrombectomy^{3, 4}. Tissue reperfusion is a stronger predictor of clinical outcome than recanalization⁵⁻⁷, but numerous adverse events may compromise reperfusion following thrombectomy, including per-procedural distal embolization, early re-occlusion, parenchymal hemorrhage (PH) and the ‘no-reflow’ phenomenon⁸.

No-reflow refers to the absence of tissue reperfusion despite complete recanalization, due to impaired microvascular perfusion. First described in rabbits following global cerebral ischemia⁹, it was subsequently confirmed in monkeys subjected to transient occlusion of the proximal middle cerebral artery (MCA)¹⁰⁻¹³ in the form of extensive areas with complete lack of capillary filling following carbon black perfusion associated with tissue infarction, as well as more recently in rodents¹⁴⁻¹⁶. No-reflow is currently believed to reflect capillary constriction secondary to pericyte disruption in previously ischemic areas^{14, 17}, possibly associated with pre-capillary small muscle cell constriction¹⁸. Disruption of capillary flow facilitates microvascular obstructions containing trapped erythrocytes and leukocytes, fibrin deposits and aggregated platelets^{14, 17, 19, 20}. Importantly, *no-reflow* may be prevented or counter-acted, for instance by acting on the NO pathway¹⁴.

Despite these experimental data, *no-reflow* remains poorly characterized in man, and while an incidence around 25% is frequently cited¹⁹, its very existence is still debated. Three main factors, which all directly derive from its definition, may explain this situation. First, documentation of complete arterial recanalization, which is afforded only by digital subtraction

angiography (DSA), is in principle required in order to reliably investigate *no-reflow*. However, DSA has only recently become part of routine acute stroke care, after thrombectomy became standard-of-care in early 2015¹. Second, complete recanalization on DSA has been variably defined over time, and a strict definition as Modified Thrombolysis in Cerebral Infarction (mTICI) score 2c or 3²¹ has only lately been widely accepted²². Third, and finally, using an imaging technique that directly assesses tissue perfusion is required to reliably evaluate reperfusion. To this day, however, no published study on *no-reflow* fulfills these three key criteria (see Discussion).

In the present proof-of-principle study, we therefore aimed to assess, in a strictly selected sample of thrombectomized LVO stroke patients with DSA-proven TICI_{2c-3} recanalization, the incidence of *no-reflow*. Based on available pre-clinical, particularly non-human primate, literature, *no-reflow* was operationally defined as severe focal hypoperfusion causing tissue infarction. Importantly, post-recanalization perfusion was evaluated by means of arterial spin labelling (ASL), a non-invasive MR-based technique that provides truly quantitative perfusion maps without the limitations of contrast agents^{23, 24} and that has been validated against conventional methods in both healthy controls and AIS patients²⁵⁻³⁰.

Methods

The data that support the findings of this study are available from the corresponding author upon reasonable request.

Operational definition of *no-reflow*

No-reflow by definition entails severe tissue hypoperfusion despite full recanalization of the previously occluded territory^{9, 10, 12, 13, 19}. For the present study, we operationally defined *no-reflow* as $\geq 40\%$ reductions in cerebral blood flow (CBF) affecting anatomical regions of the affected hemisphere on 24-hr ASL maps. This cut-off was based on a previous ASL study that demonstrated that $\geq 40\%$ CBF reduction relative to contralateral regions best identifies critical hypoperfusion, with high correlation with standard first-pass gadolinium perfusion-weighted sequence (PWI)²⁶. Anatomical regions were based on ASPECTS (Alberta Stroke Program Early CT Score)³¹, which was recently used by Yu et al to validate a score of ASL-based reperfusion after AIS³².

The other key operational component to identify *no-reflow* was tissue outcome. As *no-reflow* is consistently associated with tissue infarction^{10, 12, 13, 19}, we considered *no-reflow* to be present only if the severely hypoperfused ASPECTS area as defined above also exhibited infarction on 24hr follow-up MRI.

Study population

For the present single-center study, we retrospectively searched the Sainte-Anne Hospital prospective database of all consecutive patients treated by MT, which includes patients either directly admitted (“mothership”) or referred for MT to Sainte-Anne from other centers (“drip and ship”). As per current French regulations, prospective inclusion of patients in this database has received formal regulatory agreement. Because the present study only implied retrospective analysis of anonymized data collected as part of routine care, formal approval by an Ethics Committee was not required, but patients were offered the possibility to withdraw.

Inclusion criteria for the present study were as follows: 1/ anterior circulation AIS treated between 1/2014 and 5/2019; 2/ intracranial internal carotid artery (ICA) or first segment MCA occlusion (i.e., proximal LVO, the pre-clinical situation where *no-reflow* has been best documented^{10, 12, 13, 16}); 3/ successful recanalization by means of MT, defined as a modified TICI 2c or 3²¹ according to an experienced neuroradiologist (WBH) who reviewed the DSA dataset blinded to findings on 24hr ASL; and 4/ availability of MRI both before MT (‘MRI-1’) and ~24hr after MT (‘MRI-2’; including an ASL-sequence). Thrombolysis performed prior to MT according to international guidelines was not a cause of exclusion.

Exclusion criteria were 1/ presence on MRI-2 of parenchymal hematoma (ECASS classification³³), which may hinder assessment of ASL maps³⁴; 2/ re-occlusion, new intracranial occlusion or ipsi- or contralateral ICA or MCA $\geq 50\%$ stenosis on MRA-2, which may also affect brain perfusion; and 3/ un-interpretable ASL images due to movement artefacts, technical problems or inordinately low whole brain CBF ($<20\text{mL}/100\text{g}/\text{min}$).

Because *no-reflow* is expected to expand tissue necrosis, a secondary objective of the study was to assess MRI-1 to MRI-2 infarct growth. To limit the chance of marked pre-recanalization infarct growth, an additional exclusion criterion was MRI-1-to-groin puncture delay $\geq 3\text{hrs}$.

MRI protocol

In France, MRI is recommended as first line diagnostic imaging work-up in candidates to recanalization, and is implemented 24/7 at the Sainte-Anne comprehensive stroke center. At

Sainte-Anne hospital, a follow-up MRI (MRI-2) is carried out around 24hrs after treatment whenever feasible. All MRI data were acquired using a 1.5T MRI scanner (General Electric Healthcare). As per the above inclusion criteria, patients were included in the present study only if they had undergone both the acute and follow-up MRI sessions, and if the latter included ASL.

The following standard sequences were acquired: i) Diffusion-Weighted Imaging (DWI) with $b=0\text{s/mm}^2$ and $b=1000\text{s/mm}^2$, 6mm thick axial slices; ii) Fluid-Attenuated Inversion Recovery (FLAIR); iii) T2*, to determine the presence of haemorrhages; and iv) 3D Time-of-Flight (3D TOF) MR angiography (MRA), to determine the presence and localization of intracranial occlusion on MRI-1 and the absence of reocclusion on MRI-2. In addition, ASL perfusion maps were obtained at MRI-2 using a 3D pseudo-continuous sequence acquired using the following parameters: 4.5 minutes duration, $3.5\times 3.5\times 4\text{mm}$ resolution, TR/TE = 4600/10.5ms, pairs of control/label 3; post-labeling delay 2000ms, 40 slices with a 4.0mm thickness with whole brain coverage and background suppression, in order to suppress signal from static tissue and hence improve signal-to-noise ratio while reducing sensitivity to motion artifacts. ASL-CBF parametric perfusion maps were automatically calculated from the labelled and unlabelled ASL images (M0) with the READY VIEW® software (GE Healthcare).

Whenever feasible, MRI-1 also included a PWI sequence as well as, whenever needed, a contrast-enhanced cervical MRA to guide decision-making regarding MT.

Identification of *no-reflow on ASL Maps*

1. Visual analysis

Visual analysis was performed independently by two investigators with ASPECTS training (ATS, CP), blinded to clinical information except stroke side. Because anatomical identification may be difficult on ASL maps, the latter were rigidly co-registered to the 6mm-thick 24-hr DWI and FLAIR images, using General Electric Volume Viewer® software. Then, replicating the previously validated approach³², the investigators were instructed to select the two axial slices best matching the standard ASPECTS slices³¹, and to assess the affected hemisphere across the 10 ASPECTS regions (which have no formal boundaries³¹) for the presence of severe hypoperfusion as compared to contralateral mirror ASPECTS region. Any ASPECTS region with old infarction on MRI-1 FLAIR or hemorrhagic infarction type-2 on MRI-2 T2* was

excluded. To confirm their judgment, the investigator positioned on the co-registered DWI image a circular or elliptic two-dimensional region of interest (ROI) encompassing the hypoperfused region, and mirrored the ROI in the contralateral hemisphere. As per the operational criteria above, severe hypoperfusion was retained if mean CBF in the affected ROI was reduced $\geq 40\%$ relative to mirror ROI. Discrepancies between readers were to be resolved by consensus. As per the operational definition, any eligible ASPECTS region was then assessed for the presence of infarction on MRI-2. In addition, they were also assessed for the presence on MRI-1 of DWI hyperintense signal as well as hypoperfusion (whenever PWI was available; *no-reflow* being expected to develop in severely hypoperfused areas¹⁹).

2. Automatic analysis

To underpin the results of the visual analysis, we implemented an independent, fully quantitative and automated analysis replicating Yu et al's method³². To this end, an ASPECTS ROI template was created using the MANGO software, version 4.0.1 (Research Imaging Institute, University of Texas Health Science Center), in the T2 Montreal Neurological Institute MNI 152 space, which contains 152 axial sections each 2mm thick. In order to match the visual analysis, three contiguous MNI sections (thickness: 2mm) were selected by the first author for each of the two standard ASPECTS cuts, and the template was created by drawing the ASPECTS ROIs on each of the 6 resulting sections³², based on the AAL-2 atlas³⁵ and the study by Tatu et al³⁶.

To apply the MNI-space ASPECTS template onto each patient's ASL images, we implemented the post-processing pipeline illustrated in the **Supplemental Figure**, using Matlab R2018b (The MathWorks, Inc., Natick, MA, USA) via SPM12 (Wellcome Center for Human Imaging, UCL, UK) and the Clinical Toolbox (CRNL, University of South Carolina, USA). As initial normalization step we elected to normalize the $b=0$ maps into the Montreal Neurological Institute (MNI) space rather than directly the ASL into this space, because ASL maps are functional, as opposed to $b=0$ s/mm² being anatomical. This approach is recommended for efficient normalization³⁷. To coregister the ASL maps into MNI space, we then registered the $b=0$ s/mm² image with the M0 ASL sequence rather than the ASL derived CBF maps, as the former contains greater anatomical information. Once the ASL dataset was co-registered to the MNI 152 template, the ASPECTS ROI template was then simply projected on the six ASL slices. The CBF value for each ASPECTS region was then obtained by computing the weighted average of the CBF values of the three original ROIs belonging to this region. As with the visual

analysis, the presence of *no-reflow* was retained whenever CBF in an ipsilesional ASPECTS ROI was reduced $\geq 40\%$ relative to contralateral mirror ROI.

Clinical and imaging variables

The following data were collected:

- i) Clinical data: age, sex, vascular risk factors, history of atrial fibrillation, pre-stroke modified Rankin scale; time since last-seen-well, time of admission, National Institutes of Health Stroke Scale (NIHSS) score;
- ii) Imaging data: occlusion site (ICA, proximal or distal MCA-M1, tandem), DWI lesion site (deep or cortical) and volume for both MRI sessions: using MANGO software, DWI lesions were semi-automatically segmented, and volumes were extracted.
- iii) Thrombolysis and time of thrombolysis start, groin puncture time, mTICI score;
- iv) Cause of stroke (TOAST criteria)³⁸;
- v) NIHSS at 24hrs; early neurological improvement or deterioration (≥ 8 -point decrease in 24hr NIHSS relative to baseline or 24hr NIHSS ≤ 4 , and ≥ 4 -point increase on 24hr NIHSS, respectively^{39, 40}).
- vi) 3-month follow-up data: mRS; favourable outcome was defined as mRS ≤ 2 .

Statistical analysis

Data were analysed using SPSS Statistics Version 25 (IBM, Armonk, NY). Kappa coefficients were calculated to characterize inter-rater agreement for the visual analysis. To analyse differences between included and non-included patients, continuous variables were compared using the Wilcoxon rank-sum test, and categorical data were analysed by means of Fisher exact test. Tests were bilateral and acceptable type I error was set a priori at $\alpha=0.05$. Means are presented as mean \pm SD, medians as median (IQR).

Results

Study population

Thirty-three patients fulfilled the inclusion criteria. **Figure 1** presents the study flow-chart including the causes for exclusion. Because in our center most drip-and-ship patients return to their referring stroke center immediately following the procedure, only three drip-and-ship patients had MRI-2 including ASL in the registry; however, they were ineligible to the

present study because the delay from pre-MT MRI and groin puncture was >3hrs. Consequently, only mothership patients were included in the analysis.

The baseline characteristics, clinical and imaging data, treatment received and outcome data are summarized in **Tables 1 and 2**. Unfavorable outcome (mRS>2) was present in 12 patients. There was a significant association between unfavorable outcome and larger admission DWI lesion volume ($p = 0.001$; Mann-Whitney).

Twenty-six mothership patients with TICI 2c-3 recanalization for ICA or M1 occlusion did not undergo follow-up ASL imaging (**Figure 1**), of which 14 fulfilled the other inclusion/exclusion criteria for this study. None of the baseline and follow-up characteristics of these 14 patients significantly differed from those of the 33 included patients (**Supplemental Table 1**).

No-reflow analysis

Across the 33 included patients, eight ASPECTS regions were excluded *a priori* because of ipsilateral old infarct or hemorrhagic transformation, or contralateral old infarct ($n=3, 3$ and 2 , respectively). Accordingly, 322 ipsilateral ASPECTS regions were available for final analysis.

Visual analysis

No instance of severe focal hypoperfusion was identified in 32/33 patients. In the remaining patient, both investigators independently identified severe hypoperfusion in the same two ASPECTS regions, namely the caudate and lentiform (**Figure 2**). Inter-observer reproducibility was therefore perfect ($\kappa = 1$). Both regions were infarcted on MRI-2, and therefore fulfilled the operational criteria for *no-reflow*. Importantly, neither exhibited DWI hyperintensity on MRI-1, indicating they underwent infarction subsequently. Likewise, they did not exhibit perfusion abnormalities on baseline PWI. This patient had early neurological recovery (24-hr NIHSS=1) and excellent outcome (3-month mRS=0). Further clinical and imaging details are provided in the figure legend.

Automatic analysis

Consistent with the visual analysis, no ASPECTS ROI exhibited severe hypoperfusion in any patient save for the patient already identified with the visual analysis, involving the

caudate nucleus (CBF = -73%) but not reaching the prescribed CBF threshold for the lentiform ROI (- 22%).

Mild hypoperfusions

Given the rather unexpected finding that in our cohort *no-reflow*, as operationally defined here, was present in one patient only as compared to the widely cited prevalence of ~25%¹⁹, we carried out a *post hoc* analysis assessing milder hypoperfusions. Using the same visual analysis procedure as described above, each ASPECTS region in the affected hemispheres (saved for the two severely hypoperfused regions just described) was classified by the two independent observers into four categories, according to the presence or absence of i) hypoperfusion not fulfilling the criteria for severe hypoperfusion; and ii) infarction on concomitant DWI. The inter-observer reproducibility was again very good. Of 33 patients, 11 had at least one mildly hypoperfused ASPECTS region (**Supplemental Table 2**). Across the whole sample, 43/320 ASPECTS regions displayed mild hypoperfusion, of which two only were infarcted on MRI-2, both involving the basal ganglia in a single patient (**Figure 3**). Of note, however, both regions already showed diffusion abnormality at baseline. The remaining 41 mildly hypoperfused but non-infarcted ASPECTS regions were all cortical, except one involving the caudate.

Discussion

Consistently with both the visual and automatic analyses, there was evidence of *no-reflow*, as operationally defined in the present study, in one out of 33 patients only. This somewhat unexpected finding suggests that *no-reflow* may be a rare phenomenon, unlikely to substantially contribute to ‘futile’ recanalizations.

Supporting the above interpretation, the only patient who fulfilled the *no-reflow* criteria in our cohort had excellent outcome (mRS=0), while none of the 11 patients with poor outcome (mRS >2) did. Conversely, there was a strong association between unfavorable outcome and larger baseline DWI lesion volume, consistent with extensive previous literature⁴¹⁻⁴³. Thus, large baseline core, rather than *no-reflow*, may be the main factor accounting for futile recanalizations.

Interestingly, in the patient fulfilling the *no-reflow* operational criteria, the affected basal ganglia was not initially hypoperfused and only exhibited a small faint diffusion abnormality in the lentiform's posterior-most part, consistent with the fact that the lenticulo-striate arteries were patent on admission MRA (Fig 3). In retrospect, the clinical events prior to admission suggest initially more proximal M1 occlusion followed by spontaneous distal clot migration, resulting in clinical improvement and spontaneous reperfusion of the basal ganglia preventing extensive damage⁴⁴. Although lack of baseline hypoperfusion is unexpected for *no-reflow*, which is thought to develop in ischemic tissue¹⁹, the initial ischemic insult might have triggered delayed *no-reflow*. Two alternative mechanisms may account for basal ganglia delayed hypoperfusion and infarction in this patient, namely inadvertent occlusion of lenticulostriate arteries during, and cardio-embolic recurrence after the procedure, both implying another ischemic event rather than *no-reflow*.

The discrepancy between the visual and automatic analyses regarding this patient's lenticular nucleus can be explained by the fact that severe hypoperfusion on 24hr ASL spared its postero-lateral part (**Figure 2**), diluting the average CBF in the lentiform ASPECTS ROI used in the automatic analysis. Although the visual analysis of ASL maps has been validated against the template-based analysis³², our data suggest it is more sensitive to focal hypoperfusion not affecting entire ASPECTS ROIs.

How do our findings compare to published literature? The characteristics and findings of all 11 previously published articles that investigated impaired reperfusion despite recanalization as a surrogate for *no-reflow*^{5-7, 25, 45-51} are presented in **Table 3**. The key observation is that all the studies had significant methodological shortcomings, calling their findings into question. Thus, two studies only used DSA to assess recanalization^{45, 47}, while the rest used techniques such as transcranial Doppler, MRA or CTA, which can miss distal occlusions. Importantly, those two studies that used DSA to assess recanalization^{45, 47} unfortunately had major limitations: one defined recanalization as either partial or complete⁴⁵, and in the other DSA was used to assess reperfusion⁴⁷. Nine studies reported *no-reflow* rates of 21 to 40%, which due to these limitations may be overestimated. However, the two remaining studies, though affected by similar drawbacks, reported no instance of hypoperfusion following recanalization. In one study²⁵, hypoperfusion on 24hr ASL was present in 41/100 patients (all receiving medical treatment only), but none of these patients had complete recanalization on 24hr MRA, suggesting absence of *no-reflow* - a finding not discussed by the authors. Another study⁷ reported no instance of *no-reflow* in 13 patients with full recanalization on follow-up

MRA, but most had distal (M2) occlusions, where *no-reflow* might be difficult to detect, while reperfusion was assessed ≤ 3 hrs of admission MRI, which might be too early to reliably assess *no-reflow*. Despite these caveats, these two studies are consistent with our findings, i.e., they suggest that *no-reflow* is infrequent. Also favoring a low prevalence of *no-reflow*, another study (not listed in Table 3 as its focus wasn't on tissue reperfusion) quoted in its Methods section a rate of incomplete reperfusion in mTICI3 thrombectomized patients of 7% only⁵². The data reported in the EXTEND-IA⁵³ and DEFUSE-3⁵⁴ thrombectomy trials also appear to be consistent with a low prevalence of no-reflow: although in both reports the actual data on reperfusion after complete recanalization are missing and the latter included TICI 2b, the reported reperfusion rates were 89% and 79%, while recanalization rates were 86% and 76%, respectively.

Another piece of evidence mitigating against a high prevalence of significant *no-reflow* in our population was the negligible infarct volume growth from MRI-1 to MRI-2 (median =2 mL; Table 2), which is consistent with a recent thrombectomy study.⁵⁵ Although a portion of the acute DWI lesion may revert on 24hr follow-up MRI in some patients, it is now widely acknowledged that the latter provides a valid metric for final infarct⁵⁶.

In the present study, we considered complete recanalization as a key inclusion criterion in order to reliably assess *no-reflow*. Accordingly, only patients with TICI 2c-3 arteriographic reperfusion grades were considered eligible. As a note of caution, TICI 2c definition is “near-complete perfusion except for slow flow in a few distal cortical vessels or presence of small distal cortical emboli”, as opposed to TICI 3 which is normal angiogram^{21,22}. If one considered only TICI 3 as true complete recanalization, the incidence of *no-reflow* would be one in 11 patients, i.e. <10%. However, the lack of *no-reflow* in the 22 patients with TICI2c would be unexpected given this arteriographic grade implies poorer distal contrast clearance. Interestingly, recent studies point to no significant difference in clinical outcome between the TICI 3 and TICI 2c grades²².

An entirely different hypothesis to account for our observation would posit that *no-reflow* may exist mainly with longer occlusion times. In primates, *no-reflow* was prominent only after 3-4-hr MCA occlusion^{10, 11, 13, 57}, and it was absent following 2-hr occlusion in a rat study⁵⁸. Conversely, however, some pre-clinical studies have observed *no-reflow* as early as 1hr after occlusion^{14, 18}. Our patients received thrombectomy *as per* the mothership paradigm, and accordingly the median delay between last-time-seen-well and recanalization was relatively short, namely 208mins, although the range was wide (112 to 750min, with one outlier at

1325min). Nonetheless, *no-reflow* was rare in our standard mothership population and in turn would not account for the poor outcomes that affected one-third of our patients despite complete recanalization (Table 2).

As almost two-thirds of our patients received thrombolysis (Table 1), could t-PA have prevented *no-reflow*? To our knowledge, this issue has not been addressed experimentally, but one clinical study reported a 22% *no-reflow* incidence despite 68% of the sample receiving thrombolysis⁴⁹. Alternatively, could *no-reflow* be common only in situation of incomplete recanalization? In a thrombectomy study by Arsava et al⁵⁹, iodine contrast was injected into the distal site of occlusive thrombi prior to stent-retriever deployment, which revealed lack of capillary blush - taken to indicate microcirculatory obstructions - in 7/34 patients, all of whom subsequently had incomplete recanalization⁵⁹, suggesting that impaired microcirculatory flow might impact recanalization *per se*. However post-thrombectomy perfusion status was not assessed in this study, and the above pattern was not seen in patients who fully recanalized, making these observations of unclear relevance to the *no-reflow* phenomenon.

In the present study, presence of PH was a cause of exclusion as it would markedly hinder interpretation of 24hr perfusion maps. This is unlikely to have affected our finding, as *no-reflow* by definition prevents tissue reperfusion, and accordingly *no-reflow* was not associated with PH in primate models¹⁰⁻¹³, while one rodent study only reported associated micro-hemorrhages on pathology¹⁶. In the above-mentioned Arsava study⁵⁹, the sole PH-2 case was a patient without evidence of microcirculatory obstruction. Likewise, we excluded *a priori* all ASPECTS regions with hemorrhagic infarction type-2, which might *per se* affect regional perfusion. However, this concerned only 3 regions, none of which displayed significant hypoperfusion on *post-hoc* assessment, consistent with the established notion that hemorrhagic transformation is associated with post-recanalization *hyperperfusion*⁶⁰.

Taken together, therefore, our findings suggest that *no-reflow*, as operationally defined here, may be at best infrequent in human stroke. How can this be reconciled with the pre-clinical evidence? Given the animal, including primate, literature^{9, 10, 12, 13, 19}, where *no-reflow* is defined as markedly impaired or absent capillary perfusion, we considered severe hypoperfusion a key operational criterion to define *no-reflow*, and used as cut-off the value of 40% previously validated in earlier ASL studies as a surrogate to Tmax>6s, the validated penumbra threshold^{23, 26}. Using this definition, one patient only out of 33 with complete recanalization showed possible *no-reflow*, which prompted us to revisit *post-hoc* our dataset to assess milder hypoperfusions. Assessing milder hypoperfusions would also address the seminal observation

made by Ames et al following complete cerebral circulation arrest that lack of capillary filling involved large confluent areas interspersed with ‘mottled’ areas⁹. If mottled *no-reflow* also existed in human stroke, and considering the limited spatial resolution of ASL, it would translate as milder hypoperfusion. The results of the *post-hoc* analysis revealed that mild hypoperfusions were relatively common, with 11/33 patients showing at least one mildly hypoperfused ASPECTS region, for a total of 43 regions across the cohort. However, two such regions only were infarcted on MRI-2, both involving the basal ganglia in a single patient. Although these two regions might represent a milder form of *no-reflow*, it is important to note that they were already infarcted on admission DWI (Figure 3). This kind of mild *no-reflow* developing in already infarcted brain tissue would however have little clinical relevance.

Could mottled *no-reflow* exist without frank tissue infarction? One might raise the possibility that the penumbra rescued from infarction might be the seat of microvascular impairment as a result of either or both pre-reperfusion ischemic endothelial and pericyte damage^{17, 61} and reperfusion injury⁶², potentially causing selective neuronal loss (SNL), which has no counterpart on conventional MRI⁶³. Occurrence of SNL in the salvaged penumbra is well established histopathologically in rodent models of transient MCA occlusion⁶³, and is strongly supported by ¹¹C-flumazenil PET in stroke patients with early reperfusion⁶⁴⁻⁶⁶. However, although in rodents SNL slows down sensori-motor recovery^{67, 68}, no clinical counterpart has been documented so far in human stroke^{65, 69}. Further studies of *no-reflow* combining 24-hr ASL and delayed ¹¹C-flumazenil PET would be important to address this hypothesis.

What additional mechanisms could underly the mild hyperfusions observed on 24hr ASL maps, knowing that patients with persistent significant arterial stenosis/occlusion on 24hr MRA were *a priori* excluded from the present study? One likely mechanism is ipsilesional diaschisis, i.e., functional suppression in areas remote from but connected to the damaged area - a well-established, widely prevalent phenomenon after stroke, which frequently involves the cerebral cortex overlying deep MCA territory infarcts, so-called intra-hemispheric diaschisis⁷⁰⁻⁷². Interestingly, all 11 patients with cortical hypoperfusion in our sample had deep MCA infarcts, supporting this idea (Supplemental Table 2). To further address this hypothesis, we assessed for the presence of crossed cerebellar diaschisis (CCD), a type of diaschisis known to frequently associate with cortical diaschisis^{73, 74}. CCD was present in 6/28 patients, and was significantly more frequent in those with, as compared to those without, mildly hypoperfused cortical regions ($p=0.038$, Fisher). These findings are illustrated in Figure 3; please note also in

this patient the extension of the cortical mild hypoperfusion beyond the MCA territory, which would also favor diaschisis). Intra-hemispheric diaschisis therefore likely accounts for a substantial fraction of the mild cortical hypoperfusions observed in our cohort.

Our mechanistic study has limitations. Given the relatively small sample and retrospective design, its findings warrant confirmation in prospective cohorts. However, our cohort was extracted from a large prospective database of consecutively thrombectomized patients (Fig 1), using stringent operational criteria required to match our operational definition, notably both TICI 2c-3 recanalization and availability of 24hr ASL. As a result of our choice to replicate the only previously validated method to assess post-thrombectomy ASL maps³², severe hypoperfusion was evaluated in ASPECTS regions only. To address this potential limitation, a *post-hoc* visual analysis was carried out assessing all axial sections across the whole sample, which did not identify any additional severely hypoperfused region (data not shown). Finally, our results are applicable only to the population studied, namely mothership patients with proximal occlusion.

Summary

In our cohort of patients with proximal occlusion who enjoyed complete and stable post-thrombectomy recanalization, severe focal hypoperfusion in the affected vascular territory on 24hr follow-up imaging associated with newly developed infarction was a rare occurrence. This unexpected finding may suggest that in human stroke *no-reflow* is in fact an infrequent phenomenon that may not substantially contribute to ‘futile’ recanalizations or stand as an important therapeutic target. Prospective studies are however warranted to confirm our findings.

Acknowledgements: The authors are indebted to Ms Stéphanie Lion for expert technical assistance.

Funding: ATS received a scholarship from the Société Française Neurovasculaire (SFNV) to carry out this project as part of his MSc.

Author Contributions

AtS: conception and design of the study; acquisition and analysis of data; drafting of the manuscript and figures

SC: analysis of data; drafting a significant portion of the manuscript

WbH: data analysis

CP: data analysis

ON: acquisition and analysis of data

JB: acquisition and analysis of data

PS: data acquisition

GT: data acquisition

JCB: conception and design of the study; drafting of the manuscript and figures

CO: conception and design of the study; data acquisition; drafting a significant portion of the manuscript and figures

Disclosures: None

Supplemental information can be found on the JCBFM website

References

1. Goyal M, Menon BK, van Zwam WH, Dippel DW, Mitchell PJ, Demchuk AM *et al.* Endovascular thrombectomy after large-vessel ischaemic stroke: a meta-analysis of individual patient data from five randomised trials. *Lancet* 2016; 387(10029): 1723-31.
2. Molina CA. Futile recanalization in mechanical embolectomy trials: a call to improve selection of patients for revascularization. *Stroke* 2010; 41(5): 842-3.
3. Savitz SI, Baron JC, Yenari MA, Sanossian N, Fisher M. Reconsidering Neuroprotection in the Reperfusion Era. *Stroke* 2017; 48(12): 3413-3419.
4. Baron J-C. Protecting the ischaemic penumbra as an adjunct to thrombectomy for acute stroke. *Nature Reviews Neurology* 2018; 14(6): 325-337.
5. De Silva DA, Fink JN, Christensen S, Ebinger M, Bladin C, Levi CR *et al.* Assessing reperfusion and recanalization as markers of clinical outcomes after intravenous thrombolysis in the echoplanar imaging thrombolytic evaluation trial (EPITHET). *Stroke* 2009; 40(8): 2872-4.
6. Eilaghi A, Brooks J, d'Este C, Zhang L, Swartz RH, Lee TY *et al.* Reperfusion is a stronger predictor of good clinical outcome than recanalization in ischemic stroke. *Radiology* 2013; 269(1): 240-8.
7. Cho TH, Nighoghossian N, Mikkelsen IK, Derex L, Hermier M, Pedraza S *et al.* Reperfusion within 6 hours outperforms recanalization in predicting penumbra salvage, lesion growth, final infarct, and clinical outcome. *Stroke* 2015; 46(6): 1582-9.
8. El Amki M, Wegener S. Improving Cerebral Blood Flow after Arterial Recanalization: A Novel Therapeutic Strategy in Stroke. *Int J Mol Sci* 2017; 18(12).
9. Ames A, 3rd, Wright RL, Kowada M, Thurston JM, Majno G. Cerebral ischemia. II. The no-reflow phenomenon. *Am J Pathol* 1968; 52(2): 437-53.
10. Crowell RM, Olsson Y. Impaired microvascular filling after focal cerebral ischemia in monkeys. *J Neurosurg* 1972; 36(3): 303-9.
11. Little JR, Kerr FW, Sundt TM, Jr. Microcirculatory obstruction in focal cerebral ischemia. Relationship to neuronal alterations. *Mayo Clin Proc* 1975; 50(5): 264-70.
12. Crowell RM, Olsson Y. Impaired microvascular filling after focal cerebral ischemia in the monkey. Modification by treatment. *Neurology* 1972; 22(5): 500-4.

13. Little JR, Kerr, F.W., Sundt, T.M. Microcirculatory Obstruction in Focal Cerebral Ischemia: An Electron Microscopic Investigation in Monkeys *Stroke* 1976; 7(1): 25-30.
14. Yemisci M, Gursoy-Ozdemir Y, Vural A, Can A, Topalkara K, Dalkara T. Pericyte contraction induced by oxidative-nitrative stress impairs capillary reflow despite successful opening of an occluded cerebral artery. *Nat Med* 2009; 15(9): 1031-7.
15. Burrows FE, Bray N, Denes A, Allan SM, Schiessl I. Delayed reperfusion deficits after experimental stroke account for increased pathophysiology. *J Cereb Blood Flow Metab* 2015; 35(2): 277-84.
16. Desilles JP, Syvannarath V, Di Meglio L, Ducroux C, Boisseau W, Louedec L *et al.* Downstream Microvascular Thrombosis in Cortical Venules Is an Early Response to Proximal Cerebral Arterial Occlusion. *J Am Heart Assoc* 2018; 7(5).
17. Hall CN, Reynell C, Gesslein B, Hamilton NB, Mishra A, Sutherland BA *et al.* Capillary pericytes regulate cerebral blood flow in health and disease. *Nature* 2014; 508(7494): 55-60.
18. Hill RA, Tong L, Yuan P, Murikinati S, Gupta S, Grutzendler J. Regional Blood Flow in the Normal and Ischemic Brain Is Controlled by Arteriolar Smooth Muscle Cell Contractility and Not by Capillary Pericytes. *Neuron* 2015; 87(1): 95-110.
19. Dalkara T, Arsava EM. Can restoring incomplete microcirculatory reperfusion improve stroke outcome after thrombolysis? *J Cereb Blood Flow Metab* 2012; 32(12): 2091-9.
20. Dalkara T. Pericytes: A Novel Target to Improve Success of Recanalization Therapies. *Stroke* 2019; 50(10): 2985-2991.
21. Goyal M, Fargen KM, Turk AS, Mocco J, Liebeskind DS, Frei D *et al.* 2C or not 2C: defining an improved revascularization grading scale and the need for standardization of angiography outcomes in stroke trials. *J Neurointerv Surg* 2014; 6(2): 83-6.
22. LeCouffe NE, Kappelhof M, Treurniet KM, Lingsma HF, Zhang G, van den Wijngaard IR *et al.* 2B, 2C, or 3: What Should Be the Angiographic Target for Endovascular Treatment in Ischemic Stroke? *Stroke* 2020; 51(6): 1790-1796.
23. Zaharchuk G. Arterial spin-labeled perfusion imaging in acute ischemic stroke. *Stroke* 2014; 45(4): 1202-7.
24. Harston GW, Okell TW, Sheerin F, Schulz U, Mathieson P, Reckless I *et al.* Quantification of Serial Cerebral Blood Flow in Acute Stroke Using Arterial Spin Labeling. *Stroke* 2017; 48(1): 123-130.

25. Bivard A, Stanwell P, Levi C, Parsons M. Arterial spin labeling identifies tissue salvage and good clinical recovery after acute ischemic stroke. *J Neuroimaging* 2013; 23(3): 391-6.
26. Bivard A, Krishnamurthy V, Stanwell P, Levi C, Spratt NJ, Davis S *et al*. Arterial spin labeling versus bolus-tracking perfusion in hyperacute stroke. *Stroke* 2014; 45(1): 127-33.
27. Fan AP, Jahanian H, Holdsworth SJ, Zaharchuk G. Comparison of cerebral blood flow measurement with [15O]-water positron emission tomography and arterial spin labeling magnetic resonance imaging: A systematic review. *J Cereb Blood Flow Metab* 2016; 36(5): 842-61.
28. Huang YC, Liu HL, Lee JD, Yang JT, Weng HH, Lee M *et al*. Comparison of arterial spin labeling and dynamic susceptibility contrast perfusion MRI in patients with acute stroke. *PLoS one* 2013; 8(7): e69085.
29. Nael K, Meshksar A, Liebeskind DS, Coull BM, Krupinski EA, Villablanca JP. Quantitative analysis of hypoperfusion in acute stroke: arterial spin labeling versus dynamic susceptibility contrast. *Stroke* 2013; 44(11): 3090-6.
30. Puig O, Henriksen OM, Vestergaard MB, Hansen AE, Andersen FL, Ladefoged CN *et al*. Comparison of simultaneous arterial spin labeling MRI and (15)O-H₂O PET measurements of regional cerebral blood flow in rest and altered perfusion states. *J Cereb Blood Flow Metab* 2019: 271678X19874643.
31. Barber PA, Demchuk AM, Zhang J, Buchan AM. Validity and reliability of a quantitative computed tomography score in predicting outcome of hyperacute stroke before thrombolytic therapy. ASPECTS Study Group. Alberta Stroke Programme Early CT Score. *Lancet* 2000; 355(9216): 1670-4.
32. Yu S, Ma SJ, Liebeskind DS, Yu D, Li N, Qiao XJ *et al*. ASPECTS-based reperfusion status on arterial spin labeling is associated with clinical outcome in acute ischemic stroke patients. *J Cereb Blood Flow Metab* 2018; 38(3): 382-392.
33. Hacke W, Kaste M, Fieschi C, Toni D, Lesaffre E, von Kummer R *et al*. Intravenous thrombolysis with recombinant tissue plasminogen activator for acute hemispheric stroke. The European Cooperative Acute Stroke Study (ECASS). *JAMA* 1995; 274(13): 1017-25.
34. Tamm AS, McCourt R, Gould B, Kate M, Kosior JC, Jeerakathil T *et al*. Cerebral Perfusion Pressure is Maintained in Acute Intracerebral Hemorrhage: A CT Perfusion Study. *AJNR Am J Neuroradiol* 2016; 37(2): 244-51.
35. Rolls ET, Joliot M, Tzourio-Mazoyer N. Implementation of a new parcellation of the orbitofrontal cortex in the automated anatomical labeling atlas. *Neuroimage* 2015; 122: 1-5.

36. Tatu L, Moulin T, Bogousslavsky J, Duvernoy H. Arterial territories of the human brain: cerebral hemispheres. *Neurology* 1998; 50(6): 1699-708.
37. Ashburner J, Friston KJ. Nonlinear spatial normalization using basis functions. *Hum Brain Mapp* 1999; 7(4): 254-66.
38. Tomsick T, Broderick J, Carrozella J, Khatri P, Hill M, Palesch Y *et al.* Revascularization results in the Interventional Management of Stroke II trial. *AJNR Am J Neuroradiol* 2008; 29(3): 582-7.
39. Seners P, Turc G, Oppenheim C, Baron JC. Incidence, causes and predictors of neurological deterioration occurring within 24 h following acute ischaemic stroke: a systematic review with pathophysiological implications. *J Neurol Neurosurg Psychiatry* 2015; 86(1): 87-94.
40. Wityk RJ, Pessin MS, Kaplan RF, Caplan LR. Serial assessment of acute stroke using the NIH Stroke Scale. *Stroke* 1994; 25(2): 362-5.
41. Bivard A, Spratt N, Miteff F, Levi C, Parsons MW. Tissue Is More Important than Time in Stroke Patients Being Assessed for Thrombolysis. *Frontiers in neurology* 2018; 9: 41.
42. Marchal G, Benali K, Iglesias S, Viader F, Derlon JM, Baron JC. Voxel-based mapping of irreversible ischaemic damage with PET in acute stroke. *Brain* 1999; 122 (Pt 12): 2387-400.
43. Xie Y, Oppenheim C, Guillemin F, Gautheron V, Gory B, Raoult H *et al.* Pretreatment lesional volume impacts clinical outcome and thrombectomy efficacy. *Ann Neurol* 2018; 83(1): 178-185.
44. Olivot JM, Mlynash M, Thijs VN, Purushotham A, Kemp S, Lansberg MG *et al.* Relationships between cerebral perfusion and reversibility of acute diffusion lesions in DEFUSE: insights from RADAR. *Stroke* 2009; 40(5): 1692-7.
45. Baird AE, Donnan GA, Austin MC, Fitt GJ, Davis SM, McKay WJ. Reperfusion after thrombolytic therapy in ischemic stroke measured by single-photon emission computed tomography. *Stroke* 1994; 25(1): 79-85.
46. Yasaka M, O'Keefe GJ, Chambers BR, Davis SM, Infeld B, O'Malley H *et al.* Streptokinase in acute stroke: effect on reperfusion and recanalization. Australian Streptokinase Trial Study Group. *Neurology* 1998; 50(3): 626-32.
47. Khatri P, Neff J, Broderick JP, Khoury JC, Carrozella J, Tomsick T *et al.* Revascularization end points in stroke interventional trials: recanalization versus reperfusion in IMS-I. *Stroke* 2005; 36(11): 2400-3.

48. Soares BP, Tong E, Hom J, Cheng SC, Bredno J, Boussel L *et al.* Reperfusion is a more accurate predictor of follow-up infarct volume than recanalization: a proof of concept using CT in acute ischemic stroke patients. *Stroke* 2010; 41(1): e34-40.
49. Horsch AD, Dankbaar JW, Niesten JM, van Seeters T, van der Schaaf IC, van der Graaf Y *et al.* Predictors of reperfusion in patients with acute ischemic stroke. *AJNR Am J Neuroradiol* 2015; 36(6): 1056-62.
50. Carbone F, Busto G, Padroni M, Bernardoni A, Colagrande S, Dallegri F *et al.* Radiologic Cerebral Reperfusion at 24 h Predicts Good Clinical Outcome. *Transl Stroke Res* 2019; 10(2): 178-188.
51. Albers GW, Thijs VN, Wechsler L, Kemp S, Schlaug G, Skalabrin E *et al.* Magnetic resonance imaging profiles predict clinical response to early reperfusion: the diffusion and perfusion imaging evaluation for understanding stroke evolution (DEFUSE) study. *Ann Neurol* 2006; 60(5): 508-17.
52. Albers GW, Goyal M, Jahan R, Bonafe A, Diener HC, Levy EI *et al.* Relationships Between Imaging Assessments and Outcomes in Solitaire With the Intention for Thrombectomy as Primary Endovascular Treatment for Acute Ischemic Stroke. *Stroke* 2015; 46(10): 2786-94.
53. Campbell BC, Mitchell PJ, Kleinig TJ, Dewey HM, Churilov L, Yassi N *et al.* Endovascular Therapy for Ischemic Stroke with Perfusion-Imaging Selection. *N Engl J Med* 2015.
54. Albers GW. Thrombectomy for stroke at 6 to 16 hours with selection by perfusion imaging. *N. Engl. J. Med.* 2018.
55. Gauberti M, Lapergue B, Martinez de Lizarrondo S, Vivien D, Richard S, Bracard S *et al.* Ischemia-Reperfusion Injury After Endovascular Thrombectomy for Ischemic Stroke. *Stroke* 2018; 49(12): 3071-3074.
56. Nagaraja N, Forder JR, Warach S, Merino JG. Reversible diffusion-weighted imaging lesions in acute ischemic stroke: A systematic review. *Neurology* 2020; 94(13): 571-587.
57. Morawetz RB, DeGirolami U, Ojemann RG, Marcoux FW, Crowell RM. Cerebral blood flow determined by hydrogen clearance during middle cerebral artery occlusion in unanesthetized monkeys. *Stroke* 1978; 9(2): 143-9.
58. Li PA, Vogel J, Smith M, He QP, Kuschinsky W, Siesjo BK. Capillary patency after transient middle cerebral artery occlusion of 2 h duration. *Neurosci Lett* 1998; 253(3): 191-4.
59. Arsava EM, Arat A, Topcuoglu MA, Peker A, Yemisci M, Dalkara T. Angiographic Microcirculatory Obstructions Distal to Occlusion Signify Poor Outcome after Endovascular Treatment for Acute Ischemic Stroke. *Transl Stroke Res* 2018; 9(1): 44-50.

60. Okazaki S, Yamagami H, Yoshimoto T, Morita Y, Yamamoto H, Toyoda K *et al.* Cerebral hyperperfusion on arterial spin labeling MRI after reperfusion therapy is related to hemorrhagic transformation. *J Cereb Blood Flow Metab* 2017; 37(9): 3087-3090.
61. del Zoppo GJ, Sharp FR, Heiss WD, Albers GW. Heterogeneity in the penumbra. *J Cereb Blood Flow Metab* 2011; 31(9): 1836-51.
62. Bai J, Lyden PD. Revisiting cerebral postischemic reperfusion injury: new insights in understanding reperfusion failure, hemorrhage, and edema. *Int J Stroke* 2015; 10(2): 143-52.
63. Baron JC, Yamauchi H, Fujioka M, Endres M. Selective neuronal loss in ischemic stroke and cerebrovascular disease. *J Cereb Blood Flow Metab* 2014; 34(1): 2-18.
64. Guadagno JV, Jones PS, Aigbirhio FI, Wang D, Fryer TD, Day DJ *et al.* Selective neuronal loss in rescued penumbra relates to initial hypoperfusion. *Brain* 2008; 131(Pt 10): 2666-78.
65. Morris RS, Simon Jones P, Alawneh JA, Hong YT, Fryer TD, Aigbirhio FI *et al.* Relationships between selective neuronal loss and microglial activation after ischaemic stroke in man. *Brain* 2018; 141(7): 2098-2111.
66. Saur D, Buchert R, Knab R, Weiller C, Rother J. Iomazenil-single-photon emission computed tomography reveals selective neuronal loss in magnetic resonance-defined mismatch areas. *Stroke* 2006; 37(11): 2713-9.
67. Ejaz S, Emmrich JV, Sawiak SJ, Williamson DJ, Baron JC. Cortical selective neuronal loss, impaired behavior, and normal magnetic resonance imaging in a new rat model of true transient ischemic attacks. *Stroke* 2015; 46(4): 1084-92.
68. Sicard KM, Henninger N, Fisher M, Duong TQ, Ferris CF. Long-term changes of functional MRI-based brain function, behavioral status, and histopathology after transient focal cerebral ischemia in rats. *Stroke* 2006; 37(10): 2593-600.
69. Carrera E, Jones PS, Morris RS, Alawneh J, Hong YT, Aigbirhio FI *et al.* Is neural activation within the rescued penumbra impeded by selective neuronal loss? *Brain* 2013; 136(Pt 6): 1816-29.
70. Feeney DM, Baron JC. Diaschisis. *Stroke* 1986; 17(5): 817-30.
71. Iglesias S, Marchal G, Viader F, Baron JC. Delayed intrahemispheric remote hypometabolism. Correlations with early recovery after stroke. *Cerebrovasc Dis* 2000; 10(5): 391-402.
72. Wang C, Miao P, Liu J, Wei S, Guo Y, Li Z *et al.* Cerebral blood flow features in chronic subcortical stroke: Lesion location-dependent study. *Brain Res* 2019; 1706: 177-183.

73. Pappata S, Mazoyer B, Tran Dinh S, Cambon H, Levasseur M, Baron JC. Effects of capsular or thalamic stroke on metabolism in the cortex and cerebellum: a positron tomography study. *Stroke* 1990; 21(4): 519-24.
74. Baron JC, Bousser MG, Comar D, Castaigne P. "Crossed cerebellar diaschisis" in human supratentorial brain infarction. *Trans Am Neurol Assoc* 1981; 105: 459-61.

Figure legends:

Figure 1: Study flowchart: Abbreviations: CCA = Common Carotid Artery; ICA = Internal Carotid Artery; MCA-M1 = first segment of middle cerebral artery; MCA-M2 = second segment of the middle cerebral artery.

Figure 2: Coregistered imaging data for the single patient in whom *no-reflow* was identified. The patient had sudden-onset severe hemiparesis (three levels) and global aphasia. On admission to our hospital, the neurological deficit had partly resolved and the patient had mild 3-level hemiparesis and non-fluent dysphasia (NIHSS=4). She was treated with thrombectomy 160min after symptom onset. **(A-C)** MRI-1 obtained 84min after symptom onset, showing a small, faint DWI lesion involving the posterior-most lentiform nucleus (A, arrow), an MCA-M1 occlusion on time-of-flight angiogram (B, yellow arrow) distal to the lenticulo-striate arteries (blue arrow), and on PWI (Tmax; the pseudo-colour scale ranges from 0 to 10s) an extensive area of severe hypoperfusion covering a large part of the left cortical MCA territory (yellow arrow), but sparing the deep MCA territory (white arrow) (C). **(D)** Digital subtraction arteriography obtained immediately following thrombectomy, showing mTICI 3 recanalization. **(E-H)** 24-hr MRI-2 showing extension of the DWI lesion to the entire caudate and lentiform nuclei (E), without re-occlusion on time-of-flight MRA (F). These newly infarcted areas are severely hypoperfused on 24hrs ASL-CBF maps (G; the pseudo-colour scale is in mLs/100g.min), fulfilling the operational criteria for *no-reflow* for both regions (CBF relative to mirror region: -63% and -55%, respectively). No hemorrhage was present across the MCA territory on T2* MRI-2 (H). A,C,E,G,H: Images coregistered using GE Volume Viewer (see Methods). Stroke etiology was atrial fibrillation. This patient enjoyed early neurological recovery (24-hr NIHSS=1) and excellent outcome (3-month mRS=0).

Figure 3: Illustrative image dataset of the patient with mild hypoperfusion associated with infarction. This 66 year-old patient presented with acute-onset moderate deficit (NIHSS score = 11) and was treated with IV thrombolysis followed by thrombectomy for right terminal ICA occlusion, with mTICI 2c recanalization obtained 215min after symptom onset. Perfusion MRI was carried out prior to thrombolysis in this patient but unfortunately the data were not interpretable due to marked head motion and technical errors. **(A-C)** Illustrative DWI b=1000 sequences obtained i) on admission (68min after symptom onset) (A), and at 24hr follow-up (B and C), showing a stable DWI lesion in the striato-capsular area (i.e., deep MCA territory); **(D-F)** 24hr follow-up ASL-CBF maps, showing mild hypoperfusion within the DWI lesion (15 and 17% reduction in the caudate and lenticular nuclei, respectively, relative to contralateral ASPECTS regions; white arrows), but also cortically at distance from the DWI lesion (20-35% reduction relative to contralateral ASPECTS regions; red

arrows), spreading beyond the ICA territory (i.e., posterior circulation, yellow arrows; note that in this patient both posterior cerebral arteries originated from the basilar artery on MRA, data not shown). The left cerebellar hemisphere, i.e., contralateral to the stroke, also shows mild hypoperfusion compared to the right cerebellum (purple arrow), reflecting crossed cerebellar diaschisis. The patient made a good recovery (24hr NIHSS score = 1, 3-month mRS = 1).

Table 1: Clinical and radiological characteristics. Values shown are numbers (percentages), unless stated otherwise.

Variable	Patients (n=33)
History and characteristics at admission	
Age, years, median (IQR)	70 (61-79)
Male gender	21 (64)
Pre-stroke mRS \leq 2	31 (94)
History of hypertension	18 (55)
Current smoking	6 (18)
Atrial fibrillation	19 (58)
Stroke cause	
- Cardio-embolic	23 (70)
- Atherothrombotic	1 (3)
- Undetermined	9 (27)
Known time of symptom onset	26 (79)
Initial NIHSS score, median (IQR)	18 (12-21)
Imaging	
Stroke onset* to admission MRI delay (mins), median (IQR)	94 (72-135)
Last-time-seen-well to admission MRI delay (mins), median (IQR)	104 (72-233)
Initial perfusion imaging	23 (70)
Initial DWI lesion volume, mL, median (IQR)	10 (4-26)
Occlusion site (DSA)	
- Intracranial ICA occlusion (+/- MCA or ACA)	8 (24)
- Tandem occlusion	2 (6)
- Isolated proximal MCA-M1 occlusion	14 (42)
- Isolated distal MCA-M1 occlusion	9 (27)
Right-sided occlusion	16 (49)

mRS=modified Rankin Scale, IQR=Interquartile range; NIHSS=National Institutes of Health Stroke Scale, DWI=Diffusion Weighted Imaging, ASPECTS=Alberta Stroke Program Early CT score, ICA=Internal Carotid Artery, ACA=Anterior Carotid Artery, MCA=Middle Cerebral Artery, M1=First segment of MCA; DSA: digital subtraction angiography. *Onset of symptoms: for stroke with unknown time, time when the patient was found symptomatic.

Table 2: Treatment and follow-up data. Values shown are numbers (percentages), unless stated otherwise.

Variable	Patients (n=33)
Treatment-related data	
Intravenous thrombolysis	21 (64)
Stroke onset* to thrombolysis delay (min), median (IQR)	110 (95-144)
Stroke onset* to groin puncture delay (min), median (IQR)	150 (124-202)
Admission MRI to groin puncture delay (min), median (IQR)	52 (39-66)
First pass thrombectomy method	
- Contact aspiration	32 (97)
- Combined (contact aspiration and stent retriever)	1 (3)
Final recanalization score	
- mTICI 2c	22 (67)
- mTICI 3	11 (33)
Groin puncture to recanalization delay (min), median (IQR)	30 (16-46)
Admission MRI to recanalization delay (min), median (IQR)	84 (55-101)
Stroke onset* to recanalization delay (min), median (IQR)	196 (154-230)
Last-time-seen-well to recanalization delay (min), median (IQR)	208 (154-337)
Follow-up data	
Recanalization to follow-up MRI delay (hours), median, IQR	24 (20-27)
NIHSS at 24 hours	4 (1-9)
Δ NIHSS _{24h-initial}	11 (5-14)
Early neurological improvement [†]	26 (79)
Early neurological deterioration [‡]	0
24-hr follow-up DWI-lesion volume (mL), median (IQR)	13 (6-32)
Admission to follow-up DWI lesion volume change (mL), median (IQR)	2 (0-8)
Favorable outcome (mRS _{≤2}) at 3-months	21 (68)

IQR=Interquartile range; mTICI= modified Treatment In Cerebral Ischemia; NIHSS=National Institutes of Health Stroke Scale; mRS=modified Rankin Scale; *Onset of symptoms: for stroke with unknown time, time when the patient was found symptomatic; †: ≥ 8 -point decrease in 24hr NIHSS relative to baseline, or 24hr NIHSS ≤ 4 ; ‡: ≥ 4 -point increase on 24hr NIHSS.

Table 3: Previously published articles (listed in chronological order) on cerebral hypoperfusion in recanalized stroke patients, and present study. Methodological limitations that affect interpretation regarding the presence and reported rate of *no-reflow* appear in bold and italics.

First author, year	Acute revascularization treatment	Stroke onset to treatment delay	Recanalization assessed with	Recanalization assessment time	Definition of recanalization	Imaging modality used to assess reperfusion	Reperfusion assessment time	Number of recanalized patients	Number of recanalized patients with hypoperfusion (%)
Baird, 1994 ⁴⁵	IA SK	4-24hrs	DSA	24hrs	<i>Partial</i> † or complete	SPECT	24 hours	4	1 (25%)
Yasaka, 1998 ⁴⁶	IV SK or placebo	< 4hrs	<i>Transcranial Doppler</i> ‡	24hrs	<i>Partial</i> † or complete	SPECT	24 hours	8	4 (50%)
Khatri, 2005 ⁴⁷	IV + IA t-PA	< 3hrs	DSA	On completion of DSA	Complete (AOL III)	<i>DSA (TIMI)</i>	On DSA completion	32	26 (81%)
Albers, 2006 ⁵¹	IV t-PA	3-6hrs	<i>MRA</i> ‡	3-6hrs after t-PA	<i>Partial</i> † or complete	PWI	3-6 hours after t-PA	19	4 (21%)
DeSilva, 2009 ⁵	IV t-PA	3-6hrs	<i>MRA</i> ‡	3-5 days	<i>Partial</i> † or complete (TIMI 2-3)	PWI	3-5 days	13	4 (31%)
Soares, 2010 ⁴⁸	IV t-PA ± MT, or no treatment	< 6hrs	<i>CTA</i> ‡	24hrs	<i>Partial</i> † or complete	CTP	24 hours	13	5 (38%)
Bivard, 2013 ²⁵	IV t-PA or no treatment	< 6hrs	<i>MRA</i> ‡	24hrs	Complete	ASL	24 hours	48	0%
Eilaghi, 2013 ⁶	IV t-PA or no treatment	< 4.5hrs	<i>CTA</i> ‡	≤ 24hrs	<i>Partial</i> † or complete (TIMI 2-3)	CTP	≤ 24 hours	59	14 (24%)
Horsch, 2015 ⁴⁹	IV t-PA or no treatment	< 9hrs	<i>CTA</i> ‡	3 days	Complete	CTP	3 days	83	33 (40%)
Cho, 2015 ⁷	IV t-PA or no treatment	< 6hrs	<i>MRA</i> ‡	< 6hrs after stroke onset	<i>Partial</i> † or complete (AOL II-III)	PWI	< 6 hours of symptoms onset	13	0 (0%)
Carbone, 2019 ⁵⁰	IV t-PA ± MT, or no treatment	< 8hrs	<i>CTA</i> ‡	24hrs	<i>Partial</i> † or complete (TIMI 2-3)	CTP	24 hours	39	15 (38%)
Present study	MT ± t-PA	< 24hrs	DSA [§]	On completion of DSA	Complete (mTICI 2c-3)	ASL	24 hours	33	1 (3.3%)

‡: these techniques are inadequate to identify distal occlusions, which could in turn have caused some of the observed hypoperfusions; †: Inclusion of partial recanalization could in part account for some of the reported hypoperfusions. §: in some patients of this study (number missing), follow-up perfusion imaging was not available, in which case reperfusion was assumed to be present based on TICI 3 recanalization on completion of thrombectomy; §: lack of re-occlusion was verified in each patient using the 24hr follow-up MRA. Abbreviations: IA= Intra-arterial; IV=Intravenous; t-PA=tissue plasminogen activator; SK= streptokinase; MT= mechanical thrombectomy; DSA= digital subtraction angiography; SPECT= Single-Photon Emission Computed Tomography; AOL= Arterial Occlusive Lesion score; TIMI= Thrombolysis in Myocardial Infarction score; mTICI= modified Thrombolysis in Cerebral Infarction score; PWI=Perfusion-Weighted Imaging; MRA= Magnetic Resonance Angiography; CTA= Computed Tomography Angiography; CTP= CT perfusion

Figure 1

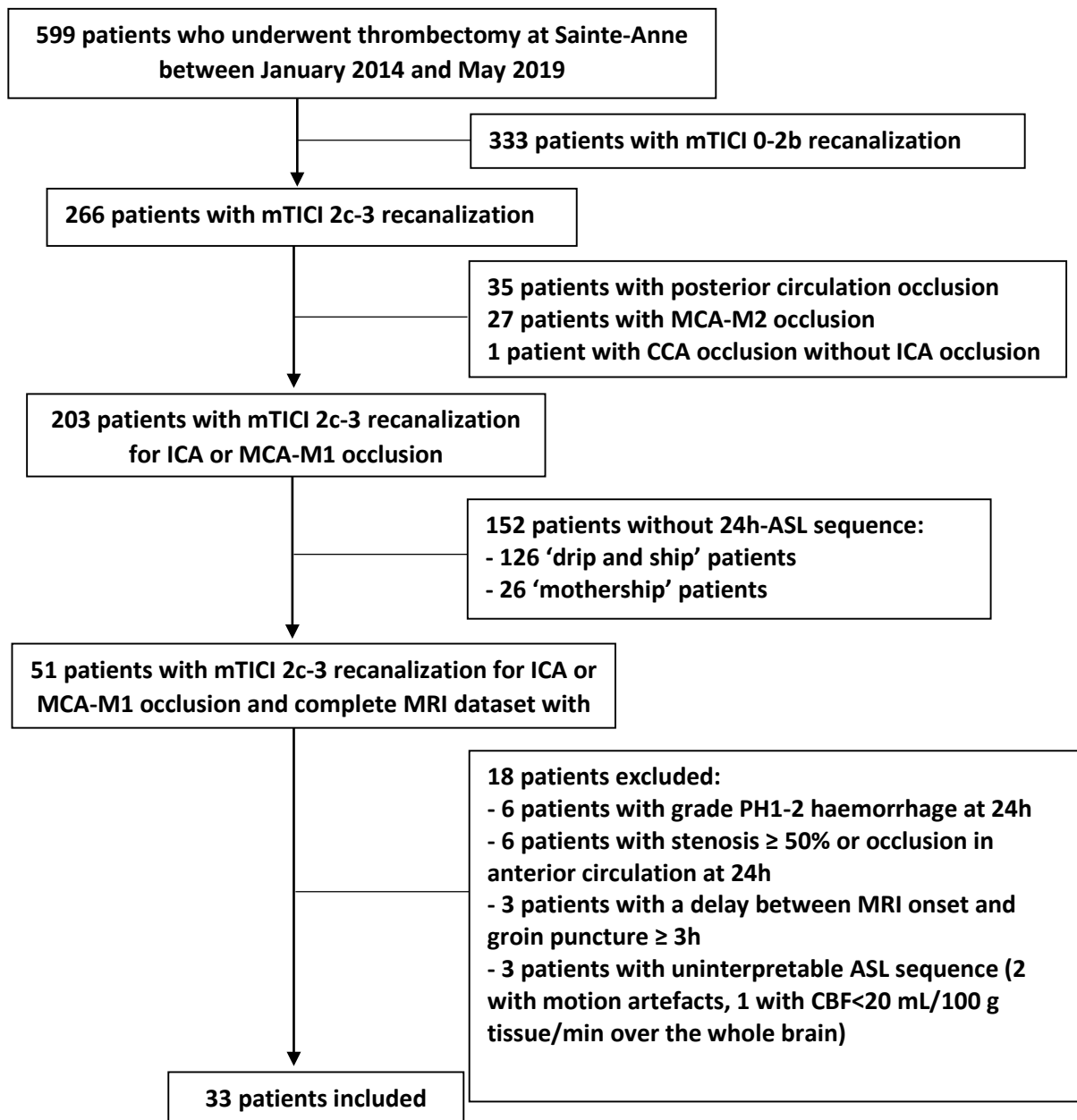


Figure 2

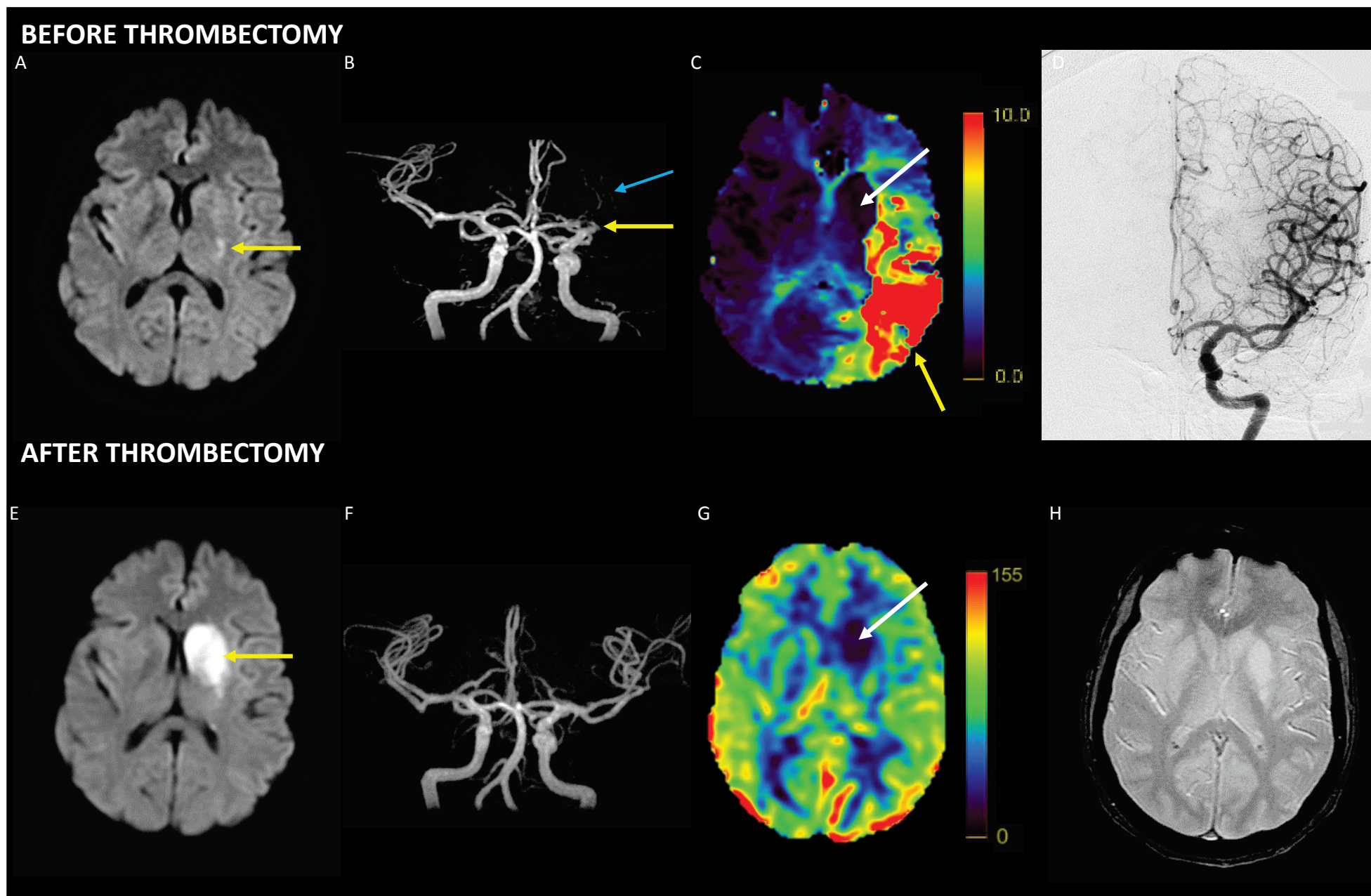
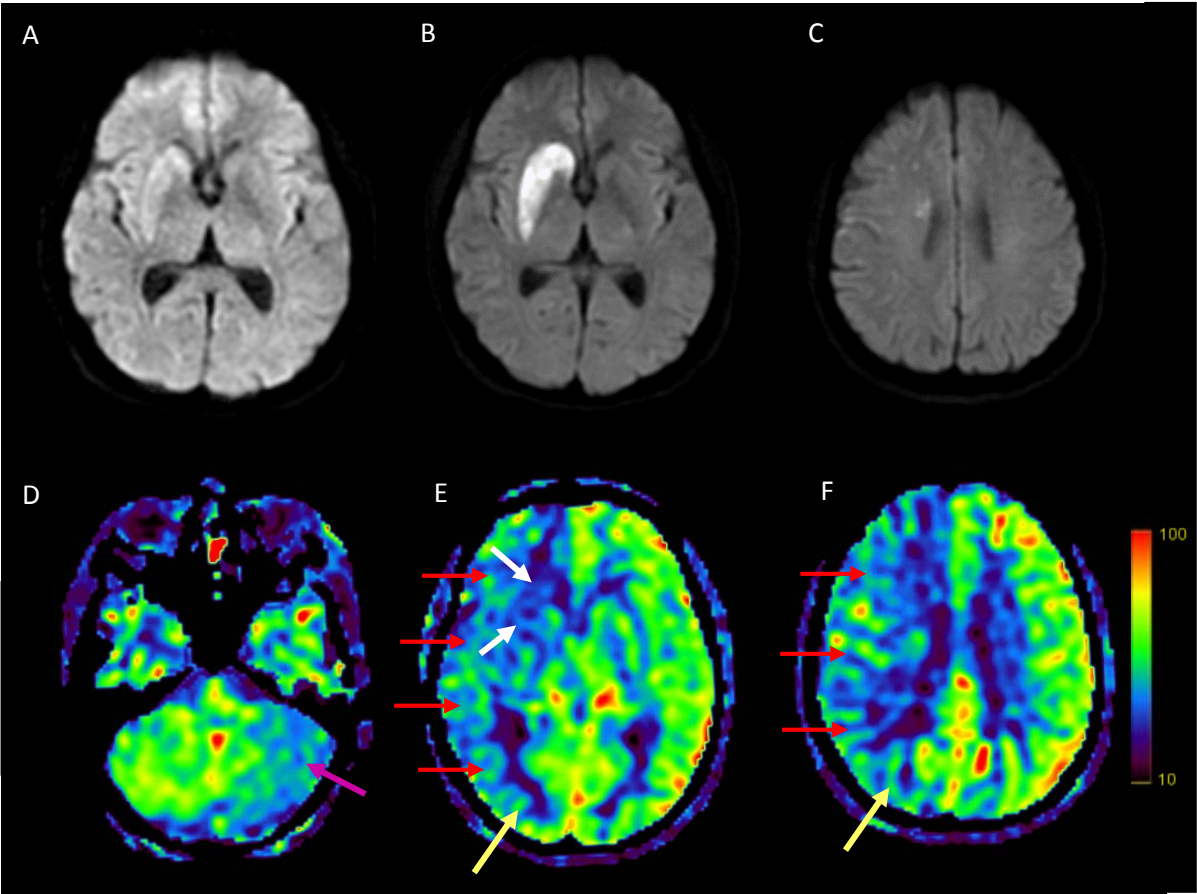


Figure 5



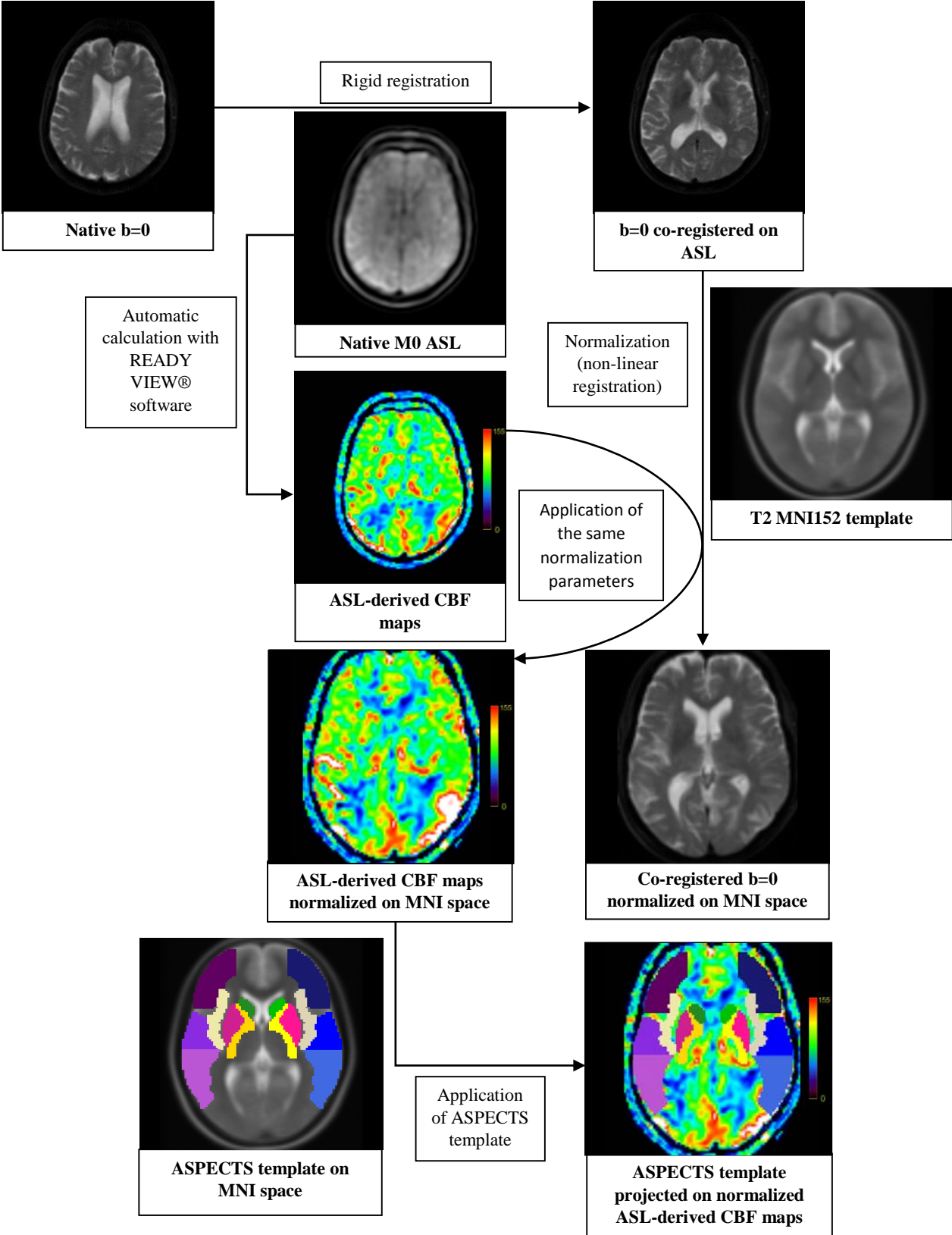
Supplemental Material

Supplemental Table 1: Comparison between the 33 included patients and the 14 mothership patients who fulfilled all inclusion/exclusion criteria except availability of 24-hr follow-up ASL (see Results for details). Values shown are numbers (percentages), unless stated otherwise.

Variable	Included patients, n=33 (%)	Patients without ASL, n=14 (%)	p
Characteristics on admission			
Age, years, median (IQR)	70 (61-79)	77 (62-84)	0.23
Male gender	21 (64)	7 (50)	0.52
Pre-stroke mRS ≤ 2	31 (94)	14 (100)	1
Initial NIHSS score, median (IQR)	18 (12-21)	19 (15-23)	0.26
Admission imaging data			
Time delay symptom onset - baseline MRI, min, median (IQR)	94 (72-135)	98 (63-116)	0.46
Thrombus localization (on arteriography)			0.46
- Intracranial ICA occlusion (+/- MCA or ACA)	8 (24)	1 (7)	
- Tandem occlusions	2 (6)	0	
- Isolated proximal MCA-M1 occlusion	14 (42)	10 (70)	
- Isolated distal MCA-M1 occlusion	9 (27)	3 (21)	
Treatment-related data			
Intravenous thrombolysis	21 (64)	8 (57)	0.75
Time delay symptom onset- thrombolysis, min, median (IQR)	110 (95-144)	140 (122-163)	0.18
Time delay symptom onset - groin puncture, min, median (IQR)	150 (124-202)	170 (118-211)	0.60
Final mTICI score 3	11 (33)	8 (57)	0.20
Time delay groin puncture – recanalization, min, median (IQR)	30 (16-46)	33 (19-66)	0.46
Follow-up data			
Time delay recanalization – follow-up imaging, hrs, median, IQR	24 (20-27)	26 (22-28)	0.31
NIHSS at 24 hours	4 (1-9)	5 (1-9)	0.41
Δ NIHSS _{24h-initial}	11 (5-14)	12 (8-14)	0.38
Early neurological improvement	26 (79)	12 (86)	0.70
Early neurological deterioration	0	0	-
Favourable prognosis (3-month mRS≤2)	21 (68)	10 (71)	0.55

ICA = Internal Carotid Artery, ACA = Anterior Carotid Artery, M1=First segment of MCA

Supplemental Figure 1: Post-processing pipeline for the automatic image analysis. First, all MRI images from both sessions were coregistered (rigid transformation) onto the native M0 ASL sequence. The coregistered DWI b=0 sequence was then spatially normalized into the Montreal Neurological Institute (MNI) space, and adequate normalization was visually verified. The same spatial normalization parameters were then applied onto the ASL-derived CBF maps (automatically calculated from native ASL images with the READY-VIEW software) so as to normalize them into the MNI 152 space. The ASPECTS ROI template was finally applied on the normalized ASL-derived CBF maps, and regional perfusion values were extracted automatically for the 10 ASPECTS ROIs and their mirror ROIs.



Supplemental Table 2: Patients with 24hr mild hypoperfusion

Patients	Age	Initial mRS	Initial NIHSS	Occlusion site	mTICI	Initial infarct location (ASPECTS)	Initial DWI-lesion volume (mL)	Final infarct location (ASPECTS)	24-hour DWI-lesion volume (mL)	24-hour mild hypoperfusion location (ASPECTS)	24-hour NIHSS	3-month mRS
1	29	0	5	M1	2C	Caudate, Insula	5.4	Caudate	8.2	M3, M4, M5, M6	0	0
2	63	0	4	M1	3	Lentiform	1.4	Caudate, Lentiform	14.1	M4	1	0
3	66	0	11	Tandem (ICA + M1)	2C	Caudate, Lentiform	9.5	Caudate, Lentiform	19.5	Caudate, Lentiform, Insula, M1, M2, M3, M4, M5, M6	1	1
4	66	0	16	M1	2C	Lentiform, M1	10.2	Lentiform, M1	7.1	Caudate, Insula, M2	3	2
5	70	0	19	M1	2C	Lentiform, Internal capsule, Insula, M1	20	Lentiform	2.2	M4, M5, M6	0	0
6	72	0	21	Intracranial ICA	3	Caudate, Lentiform, Internal capsule	3.3	Caudate, Lentiform, Internal capsule	7.7	Insula, M1, M2, M3, M4, M5, M6	6	0
7	75	0	25	M1	2C	Lentiform, Insula, M1, M2, M5	43	Lentiform, Insula, M1, M2, M5	43.4	M4, M6	20	3
8	77	1	20	M1	3	Caudate	7.8	Caudate, Lentiform	12.6	M5	4	2
9	79	0	23	Tandem (ICA + M1)	3	Caudate, Lentiform	7.4	Caudate, Lentiform, Internal capsule	21.2	M1, M2, M3, M4, M5, M6	18	2
10	85	0	19	M1	3	Lentiform	0.3	Lentiform	2.6	M1, M2, M3, M4, M5, M6	7	0
11	86	1	21	Intracranial ICA + M1)	2C	Lentiform, Insula, Internal capsule, M1	12.1	Lentiform, Insula, Internal capsule, M1	13.3	M3	8	4

Abbreviations: mTICI: modified thrombolysis in cerebral infarction score; NIHSS: National Institutes of Health Stroke Scale; mRS: modified Rankin score; MCA-M1: first segment of the middle cerebral artery; ICA: internal carotid artery; M1-M6: cortical ASPECTS regions in the middle-cerebral artery territory.